JOURNAL OF ALGEBRAIC STATISTICS
Volume 13, No. 3, 2022, p.2523-2534
https://publishoa.com
ISSN: 1309-3452

Spectroscopic Analysis of Cathode Materials ($LiNi_xMn_{2-X}O_4$) and Its Application for Lithium Ion Battery

Fikadu Boka
Physics Department, College of Natural and Computational Science, Dambi Dollo University, Dambi Dollo, Oromia Region, Ethiopia.
bokafikadu123@gmail.com

Received 2022 April 02**; Revised** 2022 May 20**; Accepted** 2022 June 18

Abstract

$LiNi_xMn_{2-x}O_4$ cathode materials were synthesized for Li-ion battery utilizing solution combustion approachwheremetalnitrates and urea as prepared sample. Characterization technique was investigated using XRD (X-Ray Diffraction), SEM (Scanning Electron Microscopy) and TGA (Thermo Gravimetric Analysis). It has been discovered that in the main yields generated incombustion methods, there was a fundamental crystalline $LiMn_2O_4$phase were present. Pure phase $LiMn_2O_4$was formed following additional annealing air in low temperature of 600^0C. Spherical morphology of synthesized sample were obtained SEM results while TGA reveal that mass is continuous decrease with temperature and it represented by the mass loss curve. The dopant of Nickel into $LiMn_2O_4$cathode materials were comparable to those reported for characterization of the electro-chemical activities among all cathode results generated by the solution ofdirect combustion technique. As a result of the research, it was discovered that $LiMn_2O_4$ derived by combustion synthesis was high potential cathode material for LIBs (lithium ion batteries).

1. Introduction

By utilizing electro-chemical redox processes, a battery can convert chemical energy stored within its electrodes into electrical power. The Lithium-ion battery (LIB) is a unique sort of secondary batteries, which can be re-chargeable for transportable power tool and electronics equipment, having slow drawback charge and high energy densities while it is not on working. It is one of the many distinct types of batteries available [1−3]. LIB is a type of battery which has three main components: cathode, electrolyte and anode. Recently lithium ion battery has many applications in manufacture of electronics such as notebooks, portable electronic devices, and mobile phones. LIB has long cycle life, high power density, and no memory effect.

$LiMn_2O_4$(LMO) spinel has low price, nice safety and environmental friend lines as well as among the most potential cathode (positive) materials, because of this it was attracted the interest of researchers[4,5]. But, there is huge problem with spinel $LiMn_2O_4$cathode material that was at elevated temperature during repeated

JOURNAL OF ALGEBRAIC STATISTICS
Volume 13, No. 3, 2022, p.2523-2534
https://publishoa.com
ISSN: 1309-3452

charge-discharge cycling it is easily capacity loss. Some of the potential causes of capacity loss in electrolyte of acidic medium may be connected to Mn dissolving inacidic-electrolytes by overstated response, gives: $2Mn^{3+} \rightarrow Mn^{2+} + Mn^{4+}$[6]. Mn^{3+} is totally released state, and lack of oxygen according to Jahn Taller. To address this issue, different investigate groups have created doped spinel materials $LiM_xMn_{2-x}O_4$ (M = Al, Ni, Fe, Co) and made strides their cyclability.$LiNi_{0.5}Mn_{1.5}O_4$ compound is characterised as an adenoidal potential cathode fabric for lithium particle batteries with a potential of roughly 4.9V [4, 7, 8].In spite of the truth that the nickel displays in spinel renders it more costly than $LiMn_2O_4$. Hence, it is basic to make strides the electrochemical behaviour of $LiMn_2O_4$ by doping these with a little amount of nickel, as expressed over, in arrange to progress its conductivity. In this inquire about; we demonstrated that doping $LiMn_2O_4$ with a 1ow concentration of nickel had a impressive affect on the execution of the fabric and increments the sum of vitality amassed and the sum of capacity.

These, lithium-ion batteries are continuously utilized at the same time as an improvement made on active density. It permits massive autonomy for a decrease weight. Completely powered airplanes by electricity are aviation by lithium ion battery. However, the existence and performance of the batteries are depends at the temperatures. To get most, efficiency the temperature of the packs ought to inside the variety. Enhance battery packs at lower fee than experimentation: numerical simulation with thermal impact is right manner to broaden lithium ion battery. The electrochemical cathode substances carry out in exclusive synthesized approach. Normally, $LiNi_xMn_{2-x}O_4$cathode materials had been synthesized the use of the technique of traditional strong-country [10,11]. However, this system necessitates the mechanical blending of lithium resources with manganese assets, that is then followed by using a excessive-temperature response. In comparison, the strong-kingdom response $LiNixMn_{2-x}O_4$spinel materials will include impurities and feature constrained manage over the stoichiometry of the reaction. As a end result, within the synthesis of substituted $LiMxMn_{2-x}O_4$ (M = Ni-doping cation) cathode substances, homogenous distribution of the cation replacement element inside the crystal lattice is considered so essential that it's been acknowledged as a critical step in the procedure. If you examine answer synthesis to solid-kingdom response, solution synthesis is more foremost since it produces a more uniform composition that contains few or no impurities. It has been mentioned that the answer synthesis of the cation-substituted $LiMn_2O_4$spinel shape may be performed through a variety of approaches, together with a sprig-drying technique [12], emulsion-drying approach [13]molten salt approach [14], and sol-gel technique [15]. Moreover, those systems involve steeply-priced reagents, time ingesting and not to be had on commercial programs. As a consequence,one among theeasy to synthesis available on industrial market is one among the answer-combustion methods (SCM)

JOURNAL OF ALGEBRAIC STATISTICS
Volume 13, No. 3, 2022, p.2523-2534
https://publishoa.com
ISSN: 1309-3452

ofwet artificial methods. In our paintings, we synthesize $LiNixMn_{2-x}O_4$cathode materials with highercapacity retention and cheap answer combustion strategies. Sphericallymorphology of cathode substances with the samedistributed micro-size debris is synthesizedand is pleasant to get more ability performance from LMOcathode materials [16, 17].As a preferred, the number one goal of this research is to synthesis and characterization of promising cathode materials ($LiNi_xMn_{2-x}O_4$) for lithium ion battery the usage of solution combustion to increase strength storage and capacity retention.

2.Experimental Details

The chemicals used in this experiment were Lithium nitrate ($LiNO_3$), Ethylene carbonate (EC), Nickel nitrate ($NiNO_3$), urea ($Co(NH_2)_2$, manganese nitrate tetra-hydrate ($Mn(NO_3)_2.H_2O$, lithium metal (50μm thick), carbon black, diethyl carbonate (DEC), lithium hex-fluorophosphates (LiPF6), and Aluminium foil (50μm thick). The equipments used in this experiment were Magnetic stirrer, Scanning Electron Microscopy (SEM), Thermo Gravimetric Analysis (TGA), Beaker, Hot plate, X-Ray Diffraction (XRD), Furnace and Grinding. The experimental procedure of this study was developed from the literature [10] a follows.$LiNO_3$ of 0.550 gm and 0.016 mol, $Mn(NO_{3)2}.4H_2O$ of 4.00 g and 0.032 mol, $Ni(NO_3)2.6H_2O$, Urea ($(NH_2)_2CO$) of 1.435 gm and 0.047 mol are the precursors that we were used in this experiment. 20.00 ml of double distilled water were needed to dissolve and the solution was kept under high speed magnetic stirrer for 30 minutes at normal temperature. The reaction was continued until the material was dissolved completely. Then after, the solution was taken to hot plate for 30 minute and combustion reactions were started. During this combustion reaction, greatest values of energy (maximum) were obtained. Here, stoichiometric calculations were occurred, by using reducing (R) and Oxidant (O) of the valences. The ratios of total oxidizing to reduction were gives unity. Atoms which were considered as reducing agents were Li, C, H, Ni and Mn with +1 Li, +4 C, +1 H, +2 Ni and +2Mn valences respectively. Oxygen atom with -2 valances was used as oxidizing agent. Pristine samples of LiMn2O4 were prepared as equation of stiochiometric below.

$LiNO_3+2Mn(NO_3)_2+4.2NH_2\text{-}CO\text{-}NH_2 \rightarrow LiMn_2O_4+6.7N_2+ 4.2CO_2+8.4H_2+3.4O_2$

Table 1 represents materials of masses with appropriate precursors based on stoichiometric calculations.These precursors were dissolved by gentle magnetic stirrer and homogeneous solutions were obtained. Then after, the solution was taken to furnace amd calcinated at 500^0C. At this stage, exothermic reactions were took place and completed at 10 minutes. Powder samples were obtained from furnace after calcinations. In preparations technique, there is some essential steps, first .boils the solutions and dehydration is occurred and decomposing was followed. Trace NO_x and other combustible like N_2H_4 and NH_3 were generated. At this stage, metal oxides were formed and in order to ignore toxic gases

JOURNAL OF ALGEBRAIC STATISTICS
Volume 13, No. 3, 2022, p.2523-2534
https://publishoa.com
ISSN: 1309-3452

extra 10 minutes were added to the reaction. After that, all of the hazardous NOx was entirely eliminated from the furnace [15]. The final step is to obtain the powder product and calcine it at 700°C for 10 hours to make the spinel crystallographic geometry of $LiMn_2O_4$. Ni was substituted with Ni ion concentrations of 0.125. 0.25, 0.375 and 0.5 mol was synthesized at700°C for 10hr. Foamy combustion and voluminous combustion ash was grounded without difficulty to obtaining cathode materials of $LiNixMn_2$-xO_4.

Table 1 Calculated stoichiometric ratio materials in gram with respected precursors

Synthesized samples	*Mass of precursor/gm*			
	$(NH_2)_2CO$	$Mn(NO_3)_{2.4}H_2O$	$LiNO_3$	$Ni(NO_3)_{2\cdot6}H_2O$
$LiMn_2O_4$	*1.435*	*4.000*	*0.550*	*0*
$LiNi_{0.125}Mn_{1.875}O_4$	*1.435*	*3.750*	*0.550*	*0.370*
$LiNi_{0.25}Mn_{1.75}O_4$	*1.435*	*3.500*	*0.550*	*0.750*
$LiNi_{0.375}Mn_{1.625}O_4$	*1.435*	*3.250*	*0.550*	*1.120*
$LiNi_{0.5}Mn_{1.5}O_4$	*1.435*	*3.000*	*0.550*	*1.500*

In next steps, 2032 coin cells were collected to gather using Li metals as anode, as a separator 2400 celgard, the solution of LiPF6 (1 mol) in 50:50 a combination of diethylene and ethylene carbonate as electrolyte [20]. Cathode were prepared by mixing active materials with powder, conducting black and vinylinedene fluoride binder in N-methyl2pyrolidone by ration of 80:10:10 respectively. Furthermore, the layer of slurry was done over aluminium foil and cured throughout night at 120 ^oC for 12 hr. 9 radius of slurry were stroked out as the cathodes. Finally, TGA (thermo-gravimetric analyzer) was used to analysis the prepared power samples.

3. Result and Discussion

Figure 1 represents the SEM image synthesized$LiNi_xMn_2$-XO_4 in terms of their structural and morphology were analyzed.SEM image also examine the morphology of as prepared of $LiMn_2O_4$, $LiNi_{0.125}Mn_{1.875}O_4$, $LiNi_{0.25}Mn_{1.85}O_4$, and $LiNi_{0.375}Mn_{1.625}O_4$.Figure 1 (a-d) displays SEM images of prepared samples of $LiMn_2O_4$, $LiNi_{0.25}Mn_{1.85}O_4$, $LiNi_{0.125}Mn_{1.875}O_4$,and $LiNi_{0.375}Mn_{1.625}O_4$ respectively. The prepared spinel of $LiNi_xMn_{2-x}O_4$ at x = 0.375, 0.25, 0.125 had spherical images. The calculated particle size was failed in the region of micrometer. During charge and discharge reaction, zero stress structure .were deviated due to spherical shaped of prepared $LiMn_2O_4$ cathode materials. Furthermore, during charge and discharge reaction distortion from Jahn Taller can countered in certain side in opposite of their morphological shapes [20- 22].The life cycle of all prepared cathode materials is due the formation of the micro-sized of the spherical shapes.The

JOURNAL OF ALGEBRAIC STATISTICS
Volume 13, No. 3, 2022, p.2523-2534
https://publishoa.com
ISSN: 1309-3452

average particle sizes calculated by Scherrer equation for the composition of x = 0.375, x = 0.25, x =0.125, and are 6.5 – 10, 4.2 – 10 μm, and 3.4 – 8 μm, respectively.

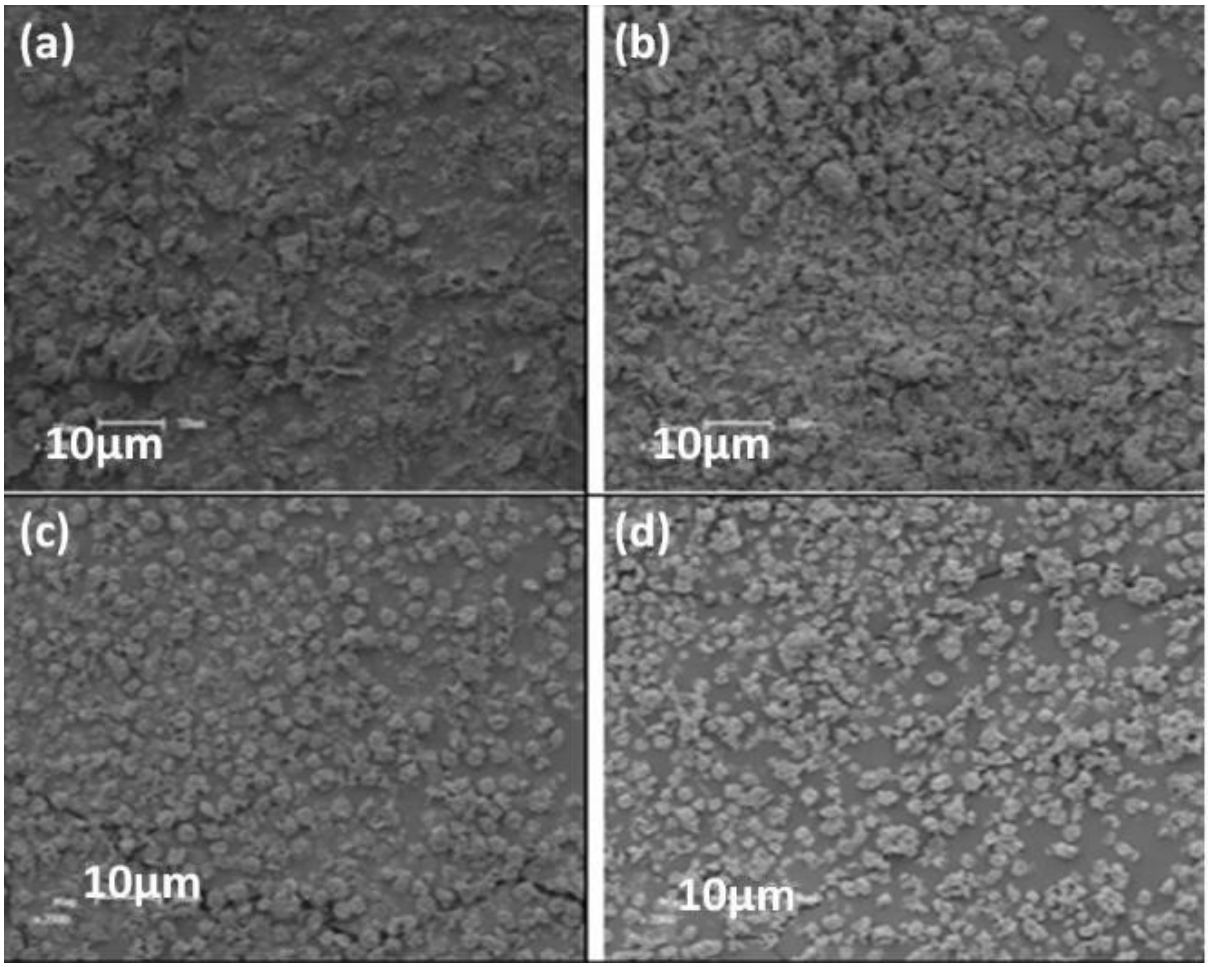

Figure 1: SEM image of the product seen from abovea) $LiMn_2O_4$ b) LiNi0.125Mn1.875O4 c) LiNi0.25Mn1.75O4 and d) LiNi0.375Mn1.625O4.

Here, the prepared $LiNi_xMn_{2-x}O_4$ crystal structures are examined by utilizing XRD. The typical XRD diffraction spectrum of as prepared micro-materials in the range of $2\theta = 0^0$- 70^0 where depicted in figure 2 below.All diffraction peaks confirms were indexed in (111), (311), (400), (511) and (440) of diffraction plane of prepared cubic structure of spinel $LiMn_2O_4$ with Fd3 m space group. The presences of impurities were reflected from the XRD results.Crystal structure were increased after Ni substitution *i.e.* Ni^{2+} ion was substituted at Mn^{3+} site in prepared $LiMn_2O_4$ cathodes materials. Therefore, no other phases were formed. Moreover, the peak of XRD graph become sharp with increasing Ni substitutions and high crystalline of the powder were observed.

JOURNAL OF ALGEBRAIC STATISTICS
Volume 13, No. 3, 2022, p.2523-2534
https://publishoa.com
ISSN: 1309-3452

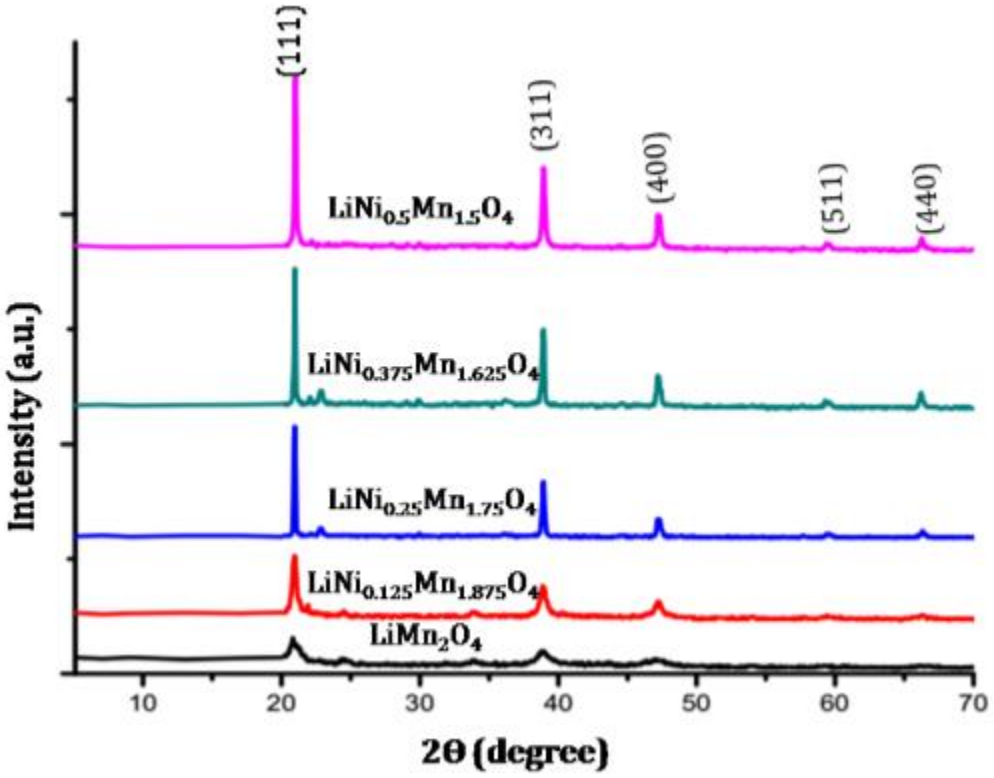

Figure 2: X-ray diffraction pattern of the prepared LiNixMn2xO4 (x = 0, 0.125, 0.25, 0.375, and 0.5) spinel cathode material.

The theoretical expressions were explained in the following [22].

$$CT = 26.8\frac{p}{M} \quad (1)$$

Where $\boldsymbol{M}$and $\boldsymbol{p}$ represents molecular weight of doped $LiMn_2O_4$,and number of Mn(III) respectively. By using eq. 1 above the theoretical output of $LiNi_xMn_{2-x}O_4$ cathode ion were 148, 132.2, 115.6, 98.3, and 80.3 mAhg-1 for x=0, x=0.125, x=0.25, x=0.375, and x=0.5, respectively. In first cycle, the discharge capacities of pristine LiNixMn2-xO4 in relation to Nicontent were explained in figure 3. There no significant difference between to discharge ability of pristine $LiMn_2O_4$ and $LiNi_{0.125}Mn_{1.875}O_4$.The lattice parameterof $LiNi_{0.125}Mn_{1.875}O_4$ is 8.3228 Å while the lattice parameter of $LiMn_2O_4$ is 8.3232 Å (see figure 3). The calculated lattice parameter is almost equal.From theoretical and experimental results, as prepared of pristine $LiMn_2O_4$ and some doped $LiNi_{0.125}Mn_{1.875}O_4$ samples displays high capacity of discharges of the first cycle and had large lattice parameter compared to other high Nickel doped samples. Li-ions can be transfer easily due to large lattice parameter and anincreased discharge capacity. At x = 0.25, 0.375 and 0.5 the first cycle of doped material is lower than that of preparation (pure $LiMn_2O$). The decrease in lattice parameter observed with high Ni-ion doping leads to lower discharge capacity.

JOURNAL OF ALGEBRAIC STATISTICS
Volume 13, No. 3, 2022, p.2523-2534
https://publishoa.com
ISSN: 1309-3452

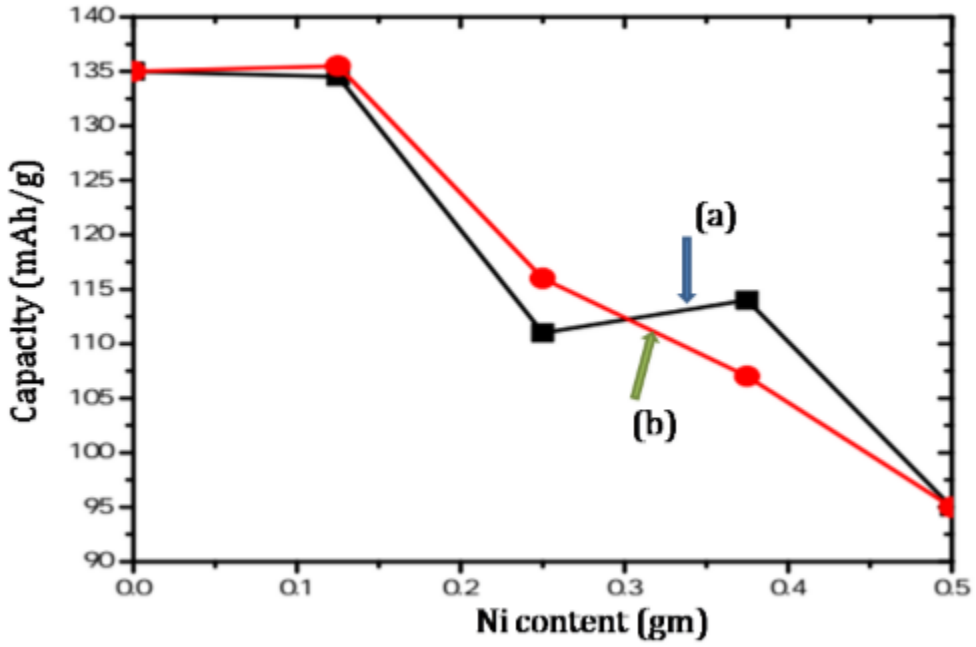

Figure 3: First cycle discharge capacity of $LiNi_xMn_{2-x}O_4$and (b) calculated lattice parameter of $LiNi_xMn_{2-x}O_4$composition (x = 0, 0.125, 0.25, 0.375, 0.5)

The charge and discharge capacity or 50th cycle output or first cycle discharge capacity of the $LiNixMn_{2-x}O_4$cathode material has been shown in Figure 4. Here, the $LiNi_{0.125}Mn_{1.875}O_4$ composition does not improve.Cyclecapacity compared with pure $LiMn_2O_4$ cathode materials while other doped materials retain their original capacity for a large number of cycles, moreover, nickel-doped compositions $LiNi_{0.25}Mn_{1.75}O_4$, $LiNi_{0.375}Mn_{1.625}O_4$and $LiNi_{0.5}Mn_{1.5}O_4$, respectively, maintain 1.5, 1.6 and 1.3 times that of pure $LiMn_2O_4$as a typical example. High retention (85%) was observed at Ni-ion concentration x = 0.375 after 50 cycles [24]. In this case, the $LiNi_{0.375}Mn_{1.625}O_4$ sample is attributed to optimal Ni-ion doping resulting in a stable spinner structure. As shown in Figure 4, as the amount of Ni-dopant increases, the amount of negatively charged interlayer energy increases, indicating that Li-ion transport is very easy.

From thermo-gravimetric analysis (TGA), a mass or mass reduction curve with temperature was analyzed. Figure 5 shows gravimetric analysis curves at a heating rate of 10°C/min in an inert atmosphere. The temperature at which the greatest mass loss is observed is determined by the first derivative of the TGA curves. The weight loss observed at 96.5°C, 494 °C and 543°C was attributed to the decomposition of functional groups and the desorption of the adsorbed water, including carboxylic and hydroxyl groups. The continuous mass loss with temperature is demonstrated from the TGA curves. A greater discharge capacity of the voltage cell is achieved when placed in a well-insulated environment or in an

JOURNAL OF ALGEBRAIC STATISTICS
Volume 13, No. 3, 2022, p.2523-2534
https://publishoa.com
ISSN: 1309-3452

adiabatic condition. Under the adiabatic condition of the first cycle discharge, the cell temperature increases at a high rate, resulting in a decrease in the diffusion limit and a higher diffusion coefficient of the binary electrolyte [25].

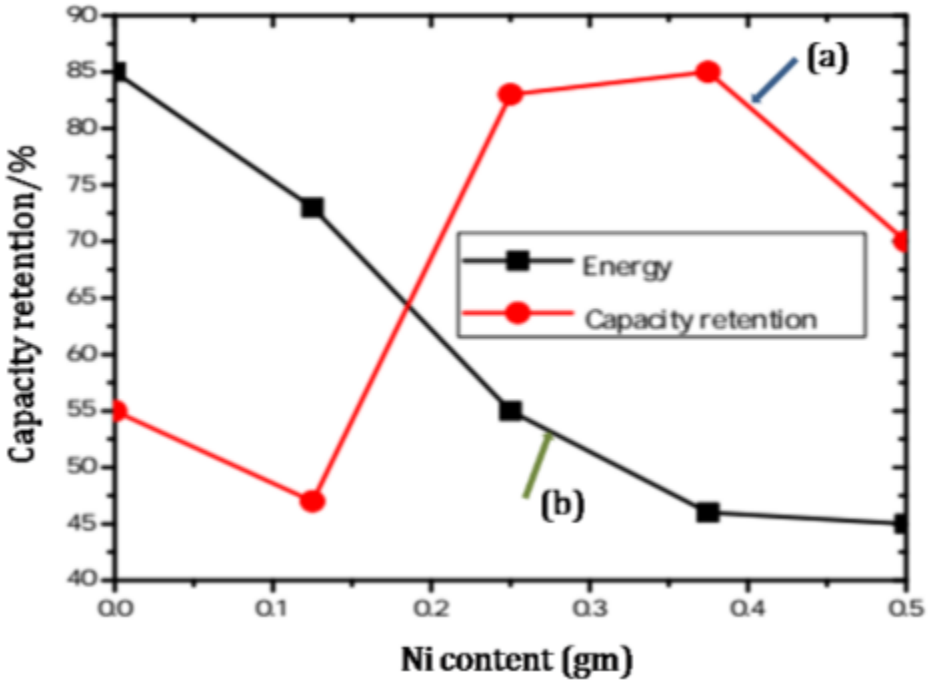

Figure 4: Retention capacity of $LiNi_xMn_{2-x}O_4$flowing after 50 cycles at C-rate = 0.2C, (b) calculated interleaving potential per Li atom

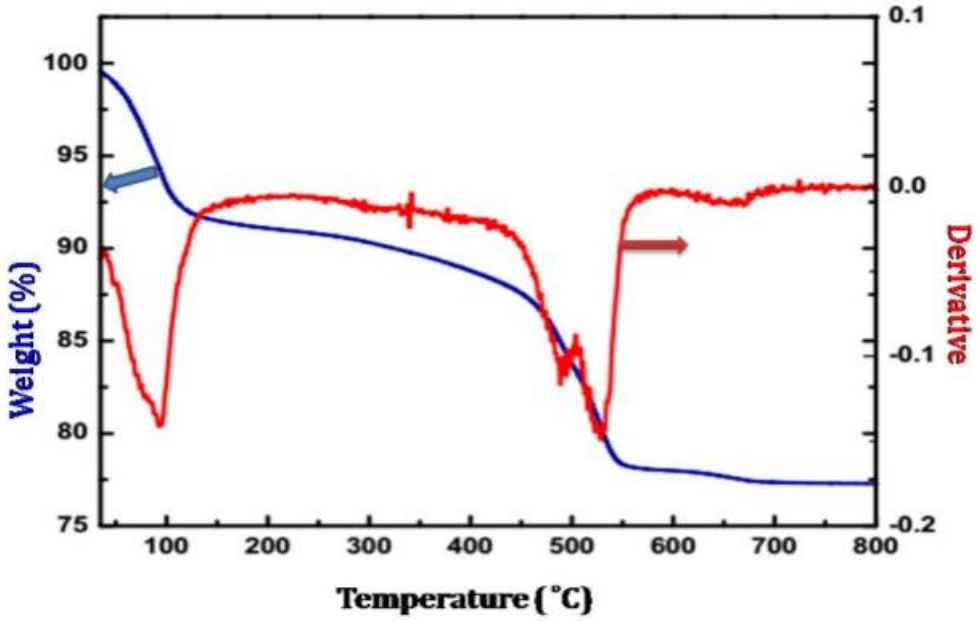

Figure: thermo-gravimetric annalistic curve at 10°C/min heating rate

JOURNAL OF ALGEBRAIC STATISTICS
Volume 13, No. 3, 2022, p.2523-2534
https://publishoa.com
ISSN: 1309-3452

A comparison of the constant discharge curves is shown in Figure 6 below. From the figure below, because of the different initial values, the first charge cycle is different from the rest, and there is a gradual decrease in the battery's voltage in each cycle.

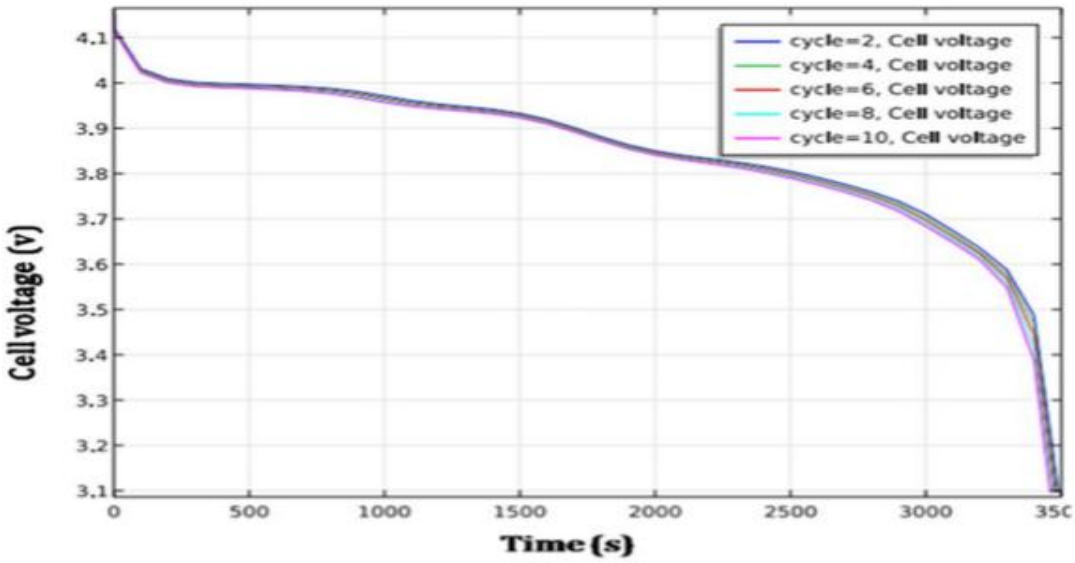

Figure 6: Battery voltage discharge current vs time comparison for cycles 2, 4, 6, 8 and 10.

Different current densities are simulated by modelling and visualization over discharges and lead to different battery discharge rates. The final charge information is obtained from this model when the cell voltage drops below 3V. The maximum discharge capacity (17.5 Ah/m^2) obtained for a current density of 1.75 Ah/m^2 (0.1C) is illustrated in figure 7 below. The results also show that the 3V discharge capacity decreases when a 1C discharge current is applied. The capacity of a C battery is about half its theoretical capacity until it reaches a cell voltage of 3V [26].

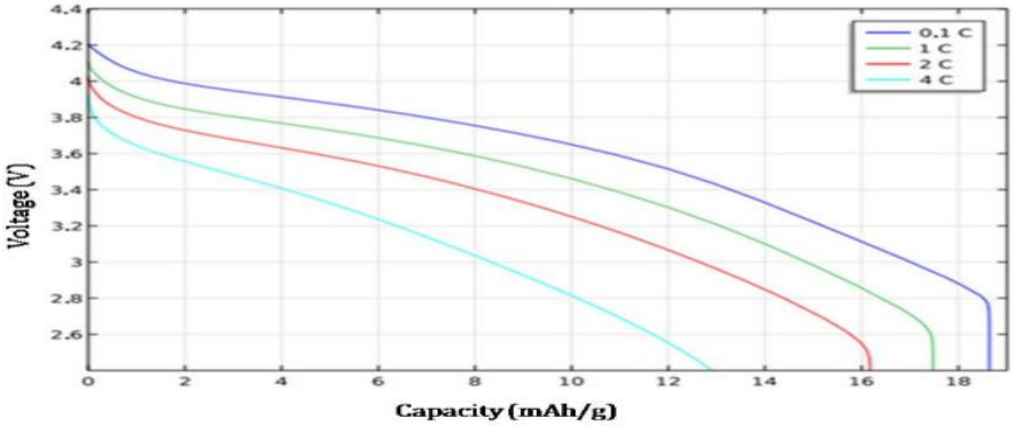

Figure 7: Discharge curves for different discharge rates.

JOURNAL OF ALGEBRAIC STATISTICS
Volume 13, No. 3, 2022, p.2523-2534
https://publishoa.com
ISSN: 1309-3452

Conclusion

The pristine spinel cathode (LMO) and Ni-doped lithium manganese oxide ($LiNi_xMn_{2-x}O_4$) materials were efficiently synthesized using a solution combustion process in which metal nitrate and urea were precursor samples.The advantage of low nickel substitution in the Spinel $LiMn_2O_4$ cathode material for lithium-ion batteries has been investigated. Sample data were characterized by battery charge/discharge tester, thermogravimetric analysis (TGA), scanning electron microscope (SEM), X-ray diffraction (XRD), as well as using COMSOL Multiphysicssoftware. The structure analyzed by SEM showed that the synthesized $LiNi_xMn_{2-x}O_4$ cathode material has a spherical shape. Examination of the X-ray diffraction patterns indicates that the powder has a high degree of crystallinity, which is evidenced by the fact that all peaks are quite sharp. The TGA curve shows the temperature at which the greatest mass reduction exists. The mass loss curve shows a continuous decrease in mass with temperature. The discharge capacity of the blank samples $LiMn_2O_4$ and $LiNi_{0.125}Mn_{1.875}O_4$did not change significantly. The higher the lattice coefficient, the easier it is for Li ions to move freely, leading to a greater discharge capacity. Compared with the pristine $LiMn_2O_4$ cathode material, the composition $LiNi_{0.125}Mn_{1.875}O_4$ does not improve the periodicity, while the other doped spinel formulations retain their inherent capabilities over the long term; for example, nickel-doped compositions $LiNi_{0.25}Mn_{1.75}O_4$, $LiNi_{0.375}Mn_{1.625}O_4$and $LiNi_{0.5}Mn_{1.5}O_4$. Moreover, compared with other samples, sample $LiNi_{0.375}Mn_{1.625}O_4$exhibits more continuous discharge capacity. In cycles from 2 to 10, the voltage of the battery gradually decreases in each cycle.

Data Availability

The data used to support the findings of this study are included within the article.

Conflicts of Interest

Authors declare that there are no conflicts of interest

Reference

[1] Le Nguyen, M., Tran, H.P., Tran, N.T. and Le, M.L.P. “Cu-doped NaCu 0.05 Fe 0.45 Co 0.5 O 2 as promising cathode material for Na-ion batteries: synthesis and characterization”. *Journal of Solid State Electrochemistry*, vol. *25*(3), pp.767-775, 2021.

[2] Bella, F., De Luca, S., Fagiolari, L., Versaci, D., Amici, J., Francia, C. and Bodoardo, S. “An overview on anodes for magnesium batteries: challenges towards a promising storage solution for renewables”. *Nanomaterials*, vol. *11*(3), pp.810, 2021.

[3] Vaughey, J., Trask, S. and Poeppelmeier, K. “Synthesis as a design variable for oxide materials”. *The Electrochemical Society Interface*, vol. *30*(1), pp.53, 2021.

[4] Akintola, T., Shellikeri, A., Akintola, T. and Zheng, J.P. “The Influence of Li4Ti5O12 Preparation Method on Lithium-Ion Capacitor Performance”. *Batteries*, vol. *7*(2), pp.33, 2021.

[5] Jia, H., Li, X., Song, J., Zhang, X., Luo, L., He, Y., Li, B., Cai, Y., Hu, S., Xiao, X. and Wang, C.“Hierarchical porous silicon

structures with extraordinary mechanical strength as high-performance lithium-ion battery anodes". *Nature communications*, vol. *11*(1), pp.1-9, 2020.

[6] Nduni, M.N., Osano, A.M. and Chaka, B. "Synthesis and characterization of aluminium oxide nanoparticles from waste aluminium foil and potential application in aluminium-ion cell". *Cleaner Engineering and Technology*, pp.100108, 2021.

[7] Yang, F., Hao, J., Long, J., Liu, S., Zheng, T., Lie, W., Chen, J. and Guo, Z. "Achieving High-Performance Metal Phosphide Anode for Potassium Ion Batteries via Concentrated Electrolyte Chemistry". *Advanced Energy Materials*, vol. *11*(6), pp.2003346, 2021.

[8] Ganas, G., Kastrinaki, G., Zarvalis, D., Karagiannakis, G., Konstandopoulos, A.G., Versaci, D. and Bodoardo, S. "Synthesis and characterization of LNMO cathode materials for lithium-ion batteries". *Materials Today: Proceedings*, vol. *5*(14), pp.27416-27424, 2018.

[9] Purwanto, A., Yudha, C.S., Ubaidillah, U., Widiyandari, H., Ogi, T. and Haerudin, H. "NCA cathode material: synthesis methods and performance enhancement efforts". *Materials Research Express*, vol. *5*(12), pp.122001, 2018.

[10] Yoon, C.S., Kim, U.H., Park, G.T., Kim, S.J., Kim, K.H., Kim, J. and Sun, Y.K. "Self-passivation of a LiNiO2 cathode for a lithium-ion battery through Zr doping". *ACS Energy Letters*, vol. *3*(7), pp.1634-1639, 2018.

[11] Shoji, M., Cheng, E.J., Kimura, T. and Kanamura, K. "Recent progress for all solid state battery using sulfide and oxide solid electrolytes". *Journal of Physics D: Applied Physics*, vol. *52*(10), pp.103001, 2019.

[12] Qiao, Y., Jiang, K., Deng, H. and Zhou, H. "A high-energy-density and long-life lithium-ion battery via reversible oxide–peroxide conversion". *Nature Catalysis*, vol. *2*(11), pp.1035-1044, 2019.

[13] Kang, Y., Zhang, Y.H., Sun, P.P., Huang, P.B., Yu, X., Shi, Q., Tian, B., Gao, J. and Shi, F.N."Bimetallic coordination polymer composites: A new choice of electrode materials for lithium ion batteries". *Solid State Ionics*, vol. *350*, pp.115310, 2020.

[14] Kang, Y., Zhang, Y.H., Shi, Q., Shi, H., Xue, D. and Shi, F.N. "Highly efficient Co3O4/CeO2 heterostructure as anode for lithium-ion batteries". *Journal of Colloid and Interface Science*, vol. *585*, pp.705-715, 2021.

[15] Xu, D., Huang, Q., Xu, X. and Sang, X. "NiMOF-derived oxygen vacancy rich NiO with excellent capacitance and ORR/OER activities as a cathode material for Zn-based hybrid batteries". *Dalton Transactions*, vol. *49*(35), pp.12441-12449, 2020.

[16] Chang, H.L., Bai, Y.W., Song, X.Y., Duan, Y.F., Sun, P.P., Tian, B., Shi, G., You, H., Gao, J. and Shi, F.N. "Hydrothermal synthesis, structural elucidation and electrochemical properties of three nickel and cobalt based phosphonates as anode materials for lithium ion batteries". *ElectrochimicaActa*, vol. *321*, pp.134647, 2019.

[17] Zhang, J., Cheng, F., Chou, S., Wang, J., Gu, L., Wang, H., Yoshikawa, H., Lu, Y. and Chen, J. "Tuning Oxygen Redox Chemistry in Li-Rich Mn-Based Layered

Oxide Cathodes by Modulating Cation Arrangement". *Advanced Materials*, vol. *31*(42), pp.1901808, 2019.

[18] Zhu, M., Li, J., Liu, Z., Wang, L., Kang, Y., Dang, Z., Yan, J. and He, X. "Preparation and Electrochemical Properties of LiNi2/3Co1/6Mn1/6O2 Cathode Material for Lithium-Ion Batteries". *Materials*, vol. *14*(7), pp.1766, 2021.

[19] Zhang, X.Y., Lin, Y.H., Hu, Y.Y. and Yang, T. "Synthesis and electrochemical performance of flexible LiFePO 4/Ti n O 2n− 1/reduced graphene oxide cathode material for lithium-ion batteries". *Ionics*, vol. *27*(5), pp.1881-1886, 2021.

[20] Çetin, B., Camtakan, Z. and Yuca, N. "Synthesis and characterization of li-rich cathode material for lithium ion batteries". *Materials Letters*, vol. *273*, pp.127927, 2020.

[21] Liu, J., Liu, Q., Zhu, H., Lin, F., Ji, Y., Li, B., Duan, J., Li, L. and Chen, Z. "Effect of different composition on voltage attenuation of Li-rich cathode material for lithium-ion batteries". *Materials*, vol. *13*(1), pp.40, 2020.

[22] Liu, J.Q., Song, S.C., Zuo, D.C., Yan, C., He, Z.J., Li, Y.J. and Zheng, J.C. "Synthesis and characterization of SiO 2/Ti 3 C 2 anode materials for lithium-ion batteries via different methods". *Ionics*, vol. *26*(11), pp.5325-5331, 2020.

[23] Chen, Q., Liu, H., Hao, J., Bi, S., Gao, C. and Chen, L. "Synthesis and characterization of high-performance RGO-modified LiNi 0.5 Mn 1.5 O 4 nanorods as a high power density cathode material for Li-ion batteries". *Ionics*, vol. *25*(1), pp.99-109, 2019.

[24] Manuel, J., Salguero, T. and Ramasamy, R.P. "Synthesis and characterization of polyanilinenanofibers as cathode active material for sodium-ion battery". *Journal of Applied Electrochemistry*, vol. *49*(5), pp.529-537, 2019.

[25] Kuganathan, N., Kordatos, A. and Chroneos, A. "Li 2 SnO 3 as a cathode material for lithium-ion batteries: defects, lithium ion diffusion and dopants". *Scientific reports*, vol. *8*(1), pp.1-9, 2018.

[26] Bergfelt, A., Lacey, M.J., Hedman, J., Sångeland, C., Brandell, D. and Bowden, T. "ε-Caprolactone-based solid polymer electrolytes for lithium-ion batteries: synthesis, electrochemical characterization and mechanical stabilization by block copolymerization". *RSC advances*, vol. *8*(30), pp.16716-16725, 2018.